Examination of zinc ferrites vs. iron oxides as contrast agents for microwave systems

Rachita Lahri[1], Mohammed Rahman[1], Javier Hernández-Gil[3], Nicholas Long[3], Panagiotis Kosmas[2], Maya Thanou[1*]
[1]Institute of Pharmaceutical Science, King's College London, London, UK, maya.thanou@kcl.ac.uk*
[2]Department of Informatics, King's College London, London, UK
[3]Department of Chemistry, Imperial College London, London, UK

***Abstract*—Iron oxide nanoparticles are biocompatible nanoparticles (NPs) that have the potential to increase the dielectric contrast of targeted tissues, hence assist in microwave imaging as a contrast agent. This study investigates the physicochemical stability and dielectric properties of iron oxide NPs. Synthesized zinc ferrites were characterised in addition to three commercial iron oxide suspensions. Zinc ferrites were synthesised using a thermal decomposition method and functionalised with a maleated polymer. The nanoparticle's characteristics were analysed for size and metal composition. Zinc ferrites showed higher dielectric contrast compared with the commercial iron oxides.**

***Index Terms*—contrast agents, dielectrics, iron oxide.**

I. Introduction

Imaging and sensing via microwave systems are gaining momentum in various medical imaging disciplines [1]–[3]. The concept relies on a non-ionising microwave source transmitting and capturing electromagnetic scattering signals from the region of interest and using an inverse scattering algorithm to produce a two-dimensional (2-D) or three-dimensional (3-D) internal map [4], which is desirable for medical imaging. Furthermore, this technique is potentially portable and inexpensive compared to current clinical standards such as MRI. Collective effort has been concentrated on breast cancer detection [5]–[8], however due to low contrast between dense tissues and the tumour [9], targeted nanoparticles (NPs) may be necessary to potentially improve the current contrast limitations.

Previous studies have shown that iron oxide nanoparticles can induce effective contrast for microwave imaging applications. Carboxylated-dextran coated iron oxide NPs were characterised at 3GHz using a cavity perturbation technique in [10], and showed that contrast in effective conductivity was caused by the colloidal stability due to the coating. Stabilised iron oxide NPs were characterised between 0.1-8GHz using a custom designed transmission line technique in [11], [12], which identified measurable magnetic contrast. Nanomaterial composites comprised of multi-wall carbon nanotubes and magnetite have demonstrated significant microwave absorption properties [13], [14] between 2-18GHz. Moreover, nickel ferrite ($NiFe_2O_4$) nanocrystals have shown high microwave absorption properties between 8.5-13GHz [15].

Superparamagnetic iron oxide nanoparticles (SPIONs) have been expansively considered for their outstanding diagnostic, practical and therapeutic applications, due to their biocompatibility capabilities [16].

In this paper, we present the synthesis and surface modification of SPIONs for dielectric contrast enhancement. Size and stability characterisation are identified, and the dielectric properties of the nanoparticles suspensions are recorded to evaluate its contrast potential. With regards to microwave diagnostic and therapeutic systems, the main finding of the paper is that zinc ferrites have non-negligible impact on the measured conductivity of water suspensions, and should be therefore studied further as possible contrast agents at microwave frequencies.

II. Materials & Methods

The materials used to synthesize iron oxide in this study are as follows; Hexadecanediol, Oleylamine, Oleic acid, Hexane, Benzyl ether, Ethanol, Poly (maleic anhydride-alt-1-octadecene) powder (PMAO), Chloroform, Sodium hydroxide, Silicone solution, and iron (III) acetylacetonate.

Three commercial iron oxide NPs were used to assess the dielectric contrast capabilities of our synthesized SPIONs. Iron oxide nanoparticles (Sienna$^+$) were obtained from Endomagnetics Ltd. These SPIONs are coated with carboxylated-dextran. The stated manufacturer size of SPIONs are known to be of size 60nm with 5nm dextran coating. Water based ferrofluids (FFs) obtained from Liquid Research Ltd. are stable colloidal dispersions of magnetic (Fe_3O_4) particles (size:$\sim$10nm) suspended in water by a dispersing agent (anionic surfactant with a carboxylate group end). Iron (II, III) oxide (Sigma) were obtained from Sigma Aldrich. Stated manufacturer size was between 50-100nm.

A. Zinc Ferrite Synthesis & Functionalisation

0.706g of Fe(acac)3 and 2.58g of hexadecandiol were added to a 50mL three neck round bottom flask along with 2.11mL of oleic acid, 2.82mL of oleylamine and 20mL of benzyl ether. The mixture was stirred and heated to 200°C for 1h and 300°C for 2h under nitrogen. At room temperature, the mixture was aliqouted with 80mL of ethanol, and was centrifuged for 30mins at 4000RPM. The supernatant was discarded and

20mL of hexane, and 50μL of oleic acid and oleylamine were added to re-suspend the pellets. The suspension was centrifuged and the pellet was discarded. Ethanol (20mL) was then added to this mixture, and left to centrifuge. The supernatant was then discarded and the remaining pellet was left to dry under vacuum overnight. The zinc ferrites were synthesized as above, however the first step was modified for each composition (Fe-SPION, Zn2-SPION & Zn4-SPION), and instead of hexadecandiol, $FeCl_2$, $Fe(acac)_3$ and $ZnCl_2$ were added as seen in Table I.

TABLE I
IRON & ZINC RATIOS IN DIFFERENT COMPOSITIONS VIA TXRF

Composition	Zn (mM)	Fe (mM)
Fe_3O_4-PMAO (Fe-SPION)	-	6.1
$Zn_{0.18}Fe_{0.82}Fe_2O_4$-PMAO (Zn2-SPION)	0.25	6.8
$Zn_{0.39}Fe_{0.61}Fe_2O_4$-PMAO (Zn4-SPION)	0.9	9

PMAO (45mg) was dissolved in 20mL of chloroform and left to stir vigorously until it dissolved. 2mg of SPIONs were added to the flask and the suspension was left to stir for 1h at room temperature. The chloroform was separated under a rotavap for 20mins at room temperature. 1mL chloroform was then added to re-dissolve the SPIONs followed by 15mL of 0.05M NaOH. The suspension was continually agitated whilst left on a hot plate set to 60°C for 10mins. 10mL NaOH was added whilst still heating and agitating the flask. This was done until a clear black solution showing no evidence of a biphasic system was produced. The solution was poured into two centrifugal filter units and centrifuged for 15mins. The NPs were removed from the filter with distilled water.

B. Dynamic Light Scattering (DLS)

Dynamic light scattering is a technique that records the averaged intensity weighted particle diameter of NPs in a suspension. Measurements were taken over time range of 4h at 6 intervals. Suspensions were prepared at concentration of 20μg/mL. Since the dielectric measurements were performed in suspensions, it was crucial to understand the macroscopic and microscopic particle interactions when in solution compared to their physical state.

C. Total Reflection X-ray Fluorescence (TXRF)

TXRF measurements were carried out with a Bruker S2 Picofox. The purpose of this excersise, was to identify the amount of zinc and iron particles in the zinc ferrite composition. 1mL of silicone solution was pipetted onto 4 numbered glass plates in petri dishes. These were then left to dry in a 60°C oven for 80mins. 2 dilutions were then prepared for each of the samples chosen (Zn2-SPIONs and Fe-SPIONs) using a gallium standard (20mg/mL). For all SPIONs, a 1:1 and a 1:10 dilution were prepared.

D. Dielectric Characterisation

In line with our previous studies [17], dispersions of 2mg/mL for each commercial iron oxide were prepared. Colloidal dispersions were made in a final volume of 20mL and 1% (v/v%) pluronic-F127 was added to the pristine iron oxide (Sigma). Samples were agitated for 2mins and sonicated for 30mins at room temperature (25°C) to ensure a complete dispersion and a homogenous solution.

Dielectric characterisation was recorded using a open-ended coaxial cable method. The slim-form probe was calibrated using three known dielectric materials; air, short block (conductive elastomer that mimics electrical properties of metal), and RO water (25°C). The minimum and maximum frequencies for the dielectric measurements was set to 1-4GHz, respectively. This range was chosen as it is the relevant frequency range for microwave tomography studies. Three different samples for each NP were prepared and five measurements per sample were taken at room temperature.

III. RESULTS & DISCUSSION

We investigated the colloidal stability and dielectric properties of commercial iron oxides; Sigma, Sienna$^+$ and FFs, dispersed in water. These NPs were used as controls against the synthesized zinc ferrites.

TABLE II
CUMULANTS ANALYSIS VIA DYNAMIC LIGHT SCATTERING

Iron oxide	Size(nm)	PDI (t_0)	PDI(t_6)
Sigma	-	0.95 $\pm$0.11	-
Sienna$^+$	64.74 $\pm$3.22	0.25 $\pm$0.02	0.24 $\pm$0.05
FFs	118.88 $\pm$27.18	0.33 $\pm$0.08	0.71 $\pm$0.12
Fe-SPION	40.21 $\pm$9.80	0.34 $\pm$0.05	0.34 $\pm$0.05
Zn2-SPION	51.35 $\pm$7.08	0.32 $\pm$0.07	0.34 $\pm$0.09
Zn4-SPION	49.68 $\pm$4.65	0.35 $\pm$0.07	0.33 $\pm$0.05

A. Stability Properties

TXRF was carried out to establish different concentrations in mM for Zn and Fe in each composition prepared. Table I shows that Zn4-SPION was prepared to have a higher concentration of zinc, which was confirmed by TXRF analysis. DLS (Table II) confirmed that Sigma NPs showed poor compatibility in water. The polydispersity index (PDI) at t_0 conveys that the particles are instantly aggregating causing large variation of particle size, while after t_6 majority of the particles sedimented. Iron oxides with bare surface tend to agglomerate due to strong magnetic attraction among particles. These particles agglomerate and form large clusters due to hydrophobic interactions between the particles, resulting in increased particle size. FFs had a PDI of 0.33 at t_0, however at t_6 large aggregates formed. The higher stability of FFs compared with Sigma can be explained by the presence of an anionic surfactant. Sienna$^+$ has high stability under DLS and the indifferent change in PDI over time suggest the high efficacy is attributed to the coating.

The three types of synthesized SPIONs show high stability over 4 hours. The difference in increased hydrodynamic size of the Zn2-SPIONs and Zn4-SPIONs compared to Fe-SPIONs would relate to the functional groups attached to the surface.

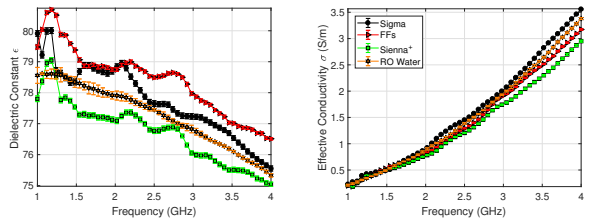

(a) Dielectric Constant ϵ (b) Effective Conductivity σ

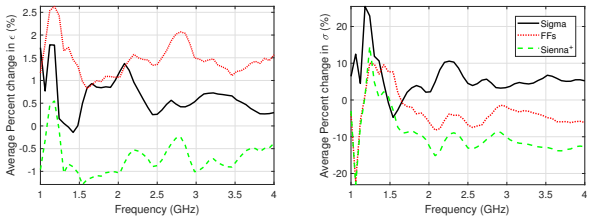

(c) $\Delta\epsilon(\%)$ (d) $\Delta\sigma(\%)$

Fig. 1. Microwave dielectric properties of commercial iron oxide (2mg/mL) suspensions (Sigma, FFs, & Sienna$^+$) recorded between 1-4GHz. (a) Dielectric constant ϵ, (b) effective conductivity σ, (c) average change in dielectric constant $\Delta\epsilon$, and (d) average change in conductivity $\Delta\sigma$.

PDI of all synthesized SPIONs barely differentiate of the final interval, suggesting high stability, suitable to be measured for dielectric properties. Suspension stability was a key factor in accurate dielectric characterisation [17], [18], and that the type of surface interactions may have an influence on its aqueous stability and integral dielectric properties [19].

B. Dielectric Analysis

The dielectric properties of commercial iron oxide dispersions have been characterised in Fig. 1 to identify contrast from the aqueous background, and to compare the dielectric contrast with our synthesized SPIONs. The contrast produced from the commercial iron oxides was insignificant. At 3GHz the dielectric constant and effective conductivity of Sigma particles were 77.23 and 1.99S/m, respectively. The dielectric contrast between the aqueous background was less than 2% over the whole frequency range. The increase in conductivity in Fig. 1(a) may be attributed to the effect of the pluronic surfactant. The surfactant was only included for Sigma suspensions to enable good dispersion for dielectric measurements. All other NPs had the required modifications for good dispersion(surfactant or polymer coating). FFs showed a maximum and minimum dielectric contrast of 2.63% and 0.82% over the whole frequency range. This change in dielectric contrast is similar to the noise level. Sienna$^+$ suspensions have a dielectric constant and effective conductivity of 76.05 and 1.74S/m, respectively at 3GHz. The dielectric contrast was $<$1%, which is insignificant. Although Sienna$^+$ are a clinically used NPs for magnetic detection, their microwave dielectric properties are not suitable for imaging/sensing. The dielectric behaviour of all 3 commercial iron oxides were extremely similar, regardless of the surfactant or the surface modifications.

Fig. 2 shows the dielectric properties of different zinc ferrites, characterised between 1-4GHz. Maximum average change in the dielectric constant was 5.4%, 3.6% and 2.35% for Zn2-SPION, Zn4-SPION and Fe-SPION respectively. Fe-SPION and Zn4-SPION showed similar dielectric contrast as the commercial iron oxide NPs. The dielectric constant Zn2-SPION at 1GHz was 82.85, in contrast to the background with 78.61. The maximum average change in effective conductivity of Zn2-SPIONs shown in Fig. 2(d) was 107.60% which is significantly higher than commercial iron oxides at 1GHz. The higher conductivity of the zinc ferrites is attributed to the Verwey's electron hopping mechanism [20]. Futhermore, polymers such as PMAO are considered to be conductive because electrons within them have the ability to jump from one chain to another, hence causing an increase within and between the chains of the polymer, hence increasing the conductivity of the medium. Decrease in the dielectric constant of the higher zinc

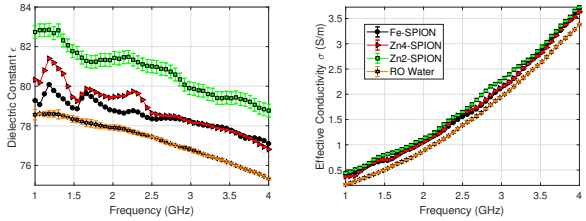

(a) Dielectric Constant ϵ (b) Effective Conductivity σ

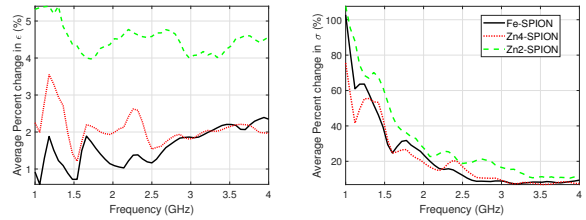

(c) $\Delta\epsilon(\%)$ (d) $\Delta\sigma(\%)$

Fig. 2. Microwave dielectric properties of synthesized iron oxide suspensions (Fe-SPION, Zn2-SPION, Zn4-SPION) recorded between 1-4GHz. (a) Dielectric constant ϵ, (b) effective conductivity σ, (c) average change in dielectric constant $\Delta\epsilon$, and (d) average change in conductivity $\Delta\sigma$.

ferrite concentration can be explained through the polarisation mechanism. Polarisation in ferrites is partially contributed by space charge polarization, and therefore a cause for the change in dielectric properties of the medium [21].

IV. Conclusion

This study shows the synthesis and evaluation of zinc ferrite particles as potential contrast enhancing materials for microwave imaging and therapeutic applications. Commercial iron oxide nanoparticles were used as controls to examine the contrast efficacy. While the dielectric contrast capabilities of the commercial iron oxides were negligible, a much stronger dielectric contrast was measured for the zinc ferrite suspensions, suggesting a potential use as microwave contrast agents.

References

[1] C. Gilmore, A. Zakaria, S. Pistorius, and J. LoVetri, "Microwave imaging of human forearms: Pilot study and image enhancement," *Intl. J. Biomed. Imaging*, vol. 2013, p. 19, 2013.

[2] P. M. Meaney, D. Goodwin, A. H. Golnabi, T. Zhou, M. Pallone, S. D. Geimer, G. Burke, and K. D. Paulsen, "Clinical microwave tomographic imaging of the calcaneus: A first-in-human case study of two subjects," *IEEE Transactions on Biomedical Engineering*, vol. 59, no. 12, pp. 3304–3313, Dec 2012.

[3] S. Ahdi Rezaeieh, A. Zamani, K. S. Bialkowski, and A. M. Abbosh, "Novel microwave torso scanner for thoracic fluid accumulation diagnosis and monitoring," *Scientific Reports*, vol. 7, no. 1, p. 304, 2017.

[4] K. Kwon, Y. Lim, C. Kim, N. Kim, C. Park, K. Yoo, S. Son, and S. Jeon, "Microwave tomography analysis system for breast tumor detection," *Journal. Med. Sys.*, vol. 36, no. 3, pp. 1757–1767, 2012.

[5] P. M. Meaney, M. W. Fanning, D. Li, S. P. Poplack, and K. D. Paulsen, "A clinical prototype for active microwave imaging of the breast," *IEEE Trans. on Microw. Theory and Tech.*, vol. 48, no. 11, pp. 1841–1853, 2000.

[6] M. Klemm, I. J. Craddock, J. A. Leendertz, A. Preece, and R. Benjamin, "Radar-based breast cancer detection using a hemispherical antenna array 2014;experimental results," *IEEE Trans. Antennas Propagat.*, vol. 57, no. 6, pp. 1692–1704, June 2009.

[7] M. Klemm, I. Craddock, J. Leendertz, A. Preece, and R. Benjamin, "Experimental and clinical results of breast cancer detection using uwb microwave radar," in *IEEE Antennas Propag. Int. Symp. AP-S 2008*, July 2008, pp. 1–4.

[8] C. Gilmore, P. Mojabi, A. Zakaria, M. Ostadrahimi, C. Kaye, S. Noghanian, L. Shafai, S. Pistorius, and J. LoVetri, "A wideband microwave tomography system with a novel frequency selection procedure," *IEEE Trans. Biomed. Eng.*, vol. 57, no. 4, pp. 894–904, April 2010.

[9] M. Lazebnik, D. Popovic, L. McCartney, C. B. Watkins, M. J. Lindstrom, J. Harter, S. Sewall, T. Ogilvie, A. Magliocco, T. M. Breslin, W. Temple, D. Mew, J. H. Booske, M. Okoniewski, and S. C. Hagness, "A large-scale study of the ultrawideband microwave dielectric properties of normal, benign and malignant breast tissues obtained from cancer surgeries," *Phys. Med. Biol.*, vol. 52, no. 20, pp. 6093–6115, 2007.

[10] O. Ogunlade and P. Beard, "Exogenous contrast agents for thermoacoustic imaging: An investigation into the underlying sources of contrast," *Med. Phys.*, vol. 42, no. 1, pp. 170–181, 2015.

[11] G. Bellizzi and O. M. Bucci, "A novel measurement technique for the broadband characterization of diluted water ferrofluids for biomedical applications," *IEEE Transactions on Magnetics*, vol. 49, no. 6, pp. 2903–2912, 2013.

[12] O. M. Bucci, G. Bellizzi, and G. G. Bellizzi, "Microwave broadband characterization of a diluted water-based ferrofluid in presence of a polarizing magnetic field," *IEEE Transactions on Magnetics*, vol. 53, no. 3, pp. 1–8, 2017.

[13] C. Zhao, A. Zhang, Y. Zheng, and J. Luan, "Electromagnetic and microwave-absorbing properties of magnetite decorated multiwalled carbon nanotubes prepared with poly(n-vinyl-2-pyrrolidone)," *Materials Research Bulletin*, vol. 47, no. 2, pp. 217–221, 2 2012.

[14] J. Qiu and T. Qiu, "Fabrication and microwave absorption properties of magnetite nanoparticle–carbon nanotube–hollow carbon fiber composites," *Carbon*, vol. 81, pp. 20–28, 2015.

[15] W. Zhu, L. Wang, R. Zhao, J. Ren, G. Lu, and Y. Wang, "Electromagnetic and microwave-absorbing properties of magnetic nickel ferrite nanocrystals," *Nanoscale*, vol. 3, no. 7, pp. 2862–2864, 2011.

[16] M.-K. Yu, Y.-Y. Jeong, J. Park, S. Park, J.-W. Kim, J.-J. Min, K. Kim, and S. Jon, "Drug-Loaded Superparamagnetic Iron Oxide Nanoparticles for Combined Cancer Imaging and Therapy In Vivo," *Angewandte Chemie International Edition*, vol. 47, no. 29, pp. 5362–5365.

[17] R. Lahri, M. Rahman, M. Wright, P. Kosmas, and M. Thanou, "Zinc oxide nanoparticles as contrast-enhancing agents for microwave imaging," *Medical Physics*, vol. 45, no. 8, pp. 3820–3830.

[18] T. Zou, H. Li, N. Zhao, and C. Shi, "Electromagnetic and microwave absorbing properties of multi-walled carbon nanotubes filled with Ni nanowire," *Journal of Alloys and Compounds*, vol. 496, no. 1, pp. L22–L24, 2010.

[19] M. W. Rahman, R. Lahri, M. Wright, M. Koutsoupidou, T. Kallos, M. Thanou, and P. Kosmas, "Characterisation of ZnO NPs as contrast agents for MWI," in *2017 International Conference on Electromagnetics in Advanced Applications (ICEAA)*, Sept 2017, pp. 1021–1024.

[20] M. Gupta and B. S. Randhawa, "Microstructural, magnetic and electric properties of mixed cs-zn ferrites prepared by solution combustion method," *Solid State Sciences*, vol. 14, no. 7, pp. 849–856, 2012.

[21] R. Rani, G. Kumar, K. M. Batoo, and M. Singh, "Electric and dielectric study of zinc substituted cobalt nanoferrites prepared by solution combustion method," *American Journal of Nanomaterials*, vol. 1, no. 1, pp. 9–12, September 2013.